

# Final Technical Report

*PI: Daniel H. Rothman, MIT*

<b>Grant title</b>	Multiphase Flow in Complex Fracture Apertures under a Wide Range of Flow Conditions
<b>Award number</b>	DE-FG07-02ER63490
<b>Project number</b>	EMSP 88516
<b>Duration</b>	September 15, 2002 - September 14, 2006.
<b>PI</b>	Daniel H. Rothman
<b>Institution</b>	Massachusetts Institute of Technology

## 1 Research objective

A better understanding of multiphase flow through fractures requires knowledge of the detailed physics of interfacial flows at the microscopic pore scale. The objective of our project was to develop tools for the simulation of such phenomena. Complementary work was performed by a group led by Dr. Paul Meakin of the Idaho National Engineering and Environmental Laboratory.

Our focus was on the lattice-Boltzmann (LB) method. In particular, we studied both the statics and dynamics of contact lines where two fluids (wetting and non-wetting) meet solid boundaries. Previous work had noted deficiencies in the way LB methods simulate such interfaces. Our work resulted in significant algorithmic improvements that alleviated these deficiencies. As a result, we were able to study in detail the behavior of the dynamic contact angle in flow through capillary tubes. Our simulations revealed that our LB method reproduces the correct scaling of the dynamic contact angle with respect to velocity, viscosity, and surface tension, without specification of an artificial slip length. Further study allowed us to identify the microscopic origin of the dynamic contact angle in LB methods. These results serve to delineate the range of applicability of multiphase LB methods to flows through complex geometries.

## 2 Research progress and implications

Progress was made in three areas. First, we identified a problem of lattice pinning in LB interface models and devised improved collision rules to solve it. Second, we showed how the improved model results in predictable static contact angles. Third, we studied in detail the behavior of dynamic contact angles when one fluid expels another that initially fills a capillary tube.

### 2.1 Lattice pinning: problem and solution

The problem of lattice pinning manifests itself in two ways: either as a microscopic bubble that does not interact with the ambient flow, or as an interface that does not move at the

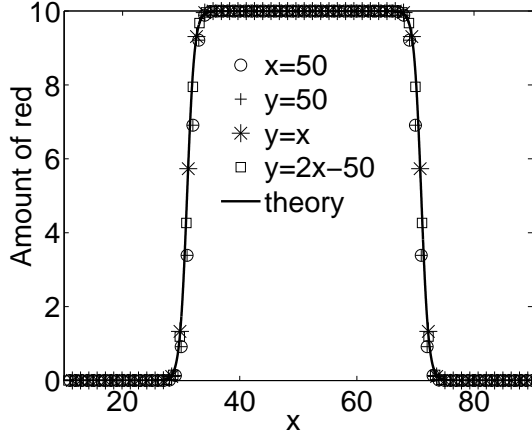


Figure 1: The interfacial curve for two-dimensional bubble. We plot the amount of the red fluid as a function of position. We have bisected the bubble in 4 different directions. The solid line is the theoretical curve derived from microscopic dynamics

correct velocity. Our work traced this problem to an approximation that had been made in the original development of two-fluid collision rules. An improvement of this approximation then effectively alleviated the problem.

The specific issue that arose concerns the way two fluids, labeled “red” and “blue,” interact microdynamically in the LB method. The original scheme relied on an *ad hoc* redistribution of color that minimized the diffusivity of color at interfaces. The improved scheme redistributes color in a systematic way according to a simple formula.

The new scheme not only improves the validity of simulations, but it is also much more easily analyzed. As a consequence we can now explicitly predict the concentration of color within the interfacial region between two fluid phases. Figure 1 shows an example.

## 2.2 Static contact angle

Another consequence of our improved microdynamics is our ability to predict the static contact angle  $\theta$  formed when the interface between wetting and nonwetting fluids is in mechanical equilibrium at a solid boundary (Figure 2). Previous work had established the existence of variable static contact angles, but the specification of the contact angle could

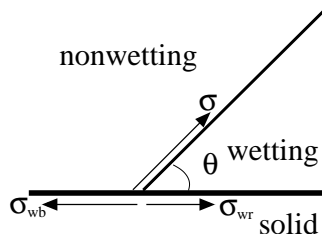


Figure 2: Force balance of the interfacial tensions  $\sigma$ ,  $\sigma_{wr}$ , and  $\sigma_{wb}$  at the three-component contact line, resulting in the static contact angle  $\theta$ .

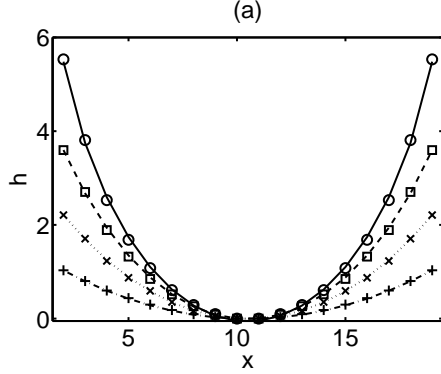


Figure 3: Equilibrium fluid-fluid interfaces resulting from capillary rise in two-dimensional tubes, for  $\cos \theta = 0.25, 0.5, 0.75$  and  $1.0$ . The curves shown are fits to circles with radii deduced from the contact angle.

only be achieved phenomenologically. With our improved model the contact angle can be derived explicitly from the microdynamical collision rules.

We tested our model by simulating capillary rise in two-dimensional and three-dimensional tubes. A balance of hydrostatic and capillary pressures predicts the capillary rise height, which increases linearly with  $\cos \theta$ . Simulations show that, unlike the original method, the improved method yields the correct equilibrium contact angle independent of initial conditions. Examples of equilibrium interfaces with different contact angles are shown in Figures 3 and 4.

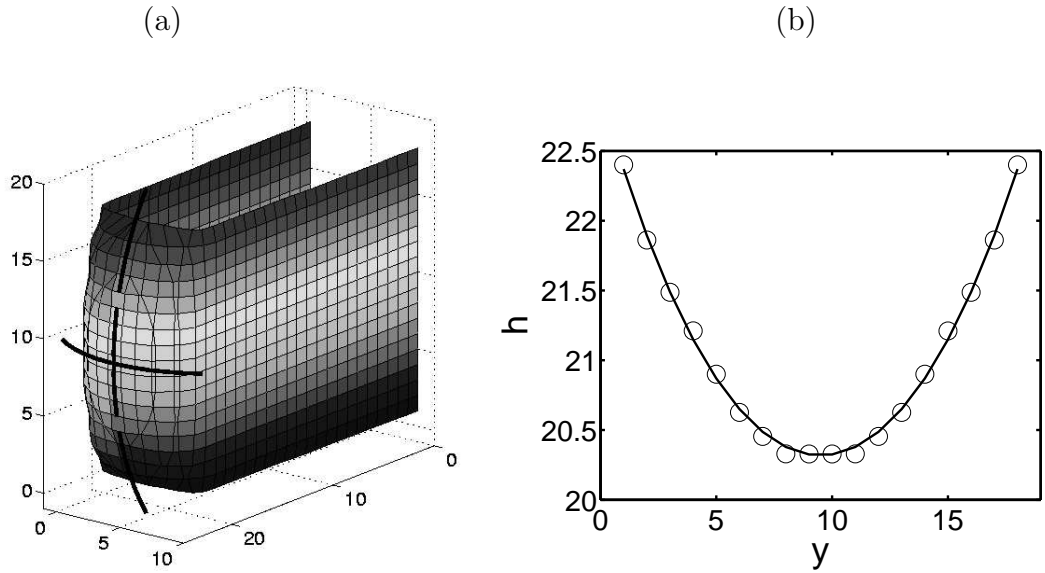


Figure 4: (a) The interface between two fluids in capillary rise through a capillary with rectangular cross-section, with  $\cos \theta = 0.5$ . (b) Detailed comparison of the theoretically predicted equilibrium interface (smooth curve) and the simulation (circles).

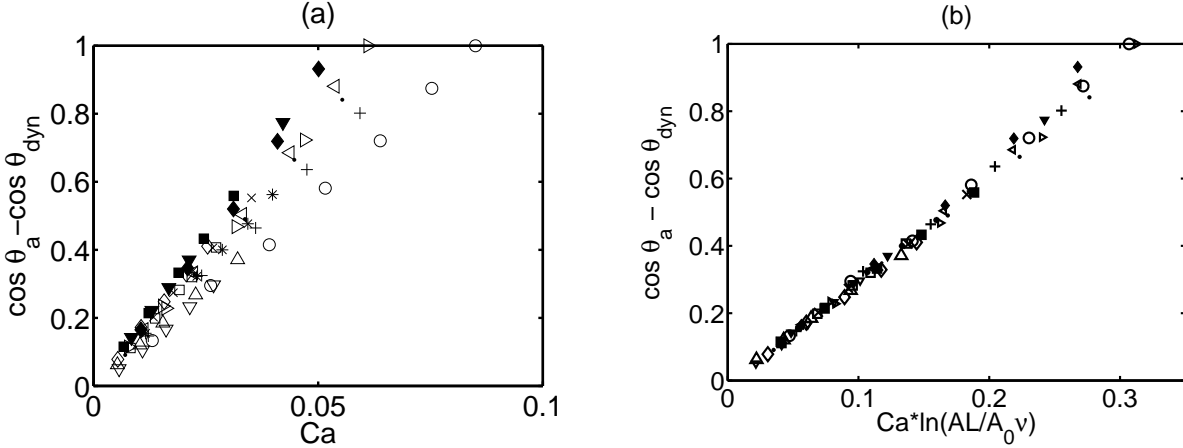


Figure 5: (a) The dynamic contact angle as a function of capillary number  $Ca$ . (b) The same data rescaled as a function of  $Ca \ln(AL/A_0\nu)$ , where  $A$  proportional to the surface tension,  $L$  is the width of the rectangular capillary tube,  $\nu$  is the kinematic viscosity, and  $A_0$  is a constant fitting parameter. The data points give the measured dynamic contact angle in LB simulations. The markers indicate different values of  $A$ ,  $\nu$  and  $L$ .

### 2.3 Dynamic contact angle

The work summarized above enabled us to address a long-standing conundrum in fluid dynamics: the motion of contact lines at solid surfaces, despite the presumed validity of the “no-slip” boundary condition. We studied this problem in the context of lattice-Boltzmann models.

Models of moving contact lines distinguish between an *advancing contact angle*,  $\theta_a$ , and a *dynamic contact angle*,  $\theta_{dyn}$ . Decades of work have shown that the difference between the two is a function of the capillary number  $Ca$ . The situation is illustrated by the results of lattice Boltzmann simulations shown in Figure 5. As expected, the dynamic contact angle increases as capillary number increases. For any given set of the simulation parameters, the excess curvature  $\cos \theta_a - \cos \theta_{dyn}$  depends linearly on the capillary number. However if any of the simulation parameters change the proportionality factor also changes. These curves collapse to a single line if one instead plots  $\cos \theta_a - \cos \theta_{dyn}$  as a function of  $Ca \ln(AL/A_0\nu)$ , where  $A$  is a parameter proportional to the surface tension,  $L$  is the width of the rectangular capillary tube,  $\nu$  is the kinematic viscosity, and  $A_0$  is a constant fitting parameter. The quantity  $\nu A_0 / A$  plays the role of a *slip length* as employed in the classical Navier slip model. However this slip length is not specified in the LB model—it instead emerges naturally from the LB microdynamics.

How does the contact line move without specification of a slip length? To gain a better understanding, we investigated the lattice dynamics near the three phase contact point. At corner sites (i.e. sites neighboring both the wall and the fluid-fluid interface) particle populations are perturbed in a way that introduces stress to fluid elements. This stress mimics the surface tension for flat and moderately curved interfaces. However at the corner node the stress changes abruptly in a way that cannot be compensated by an increase in

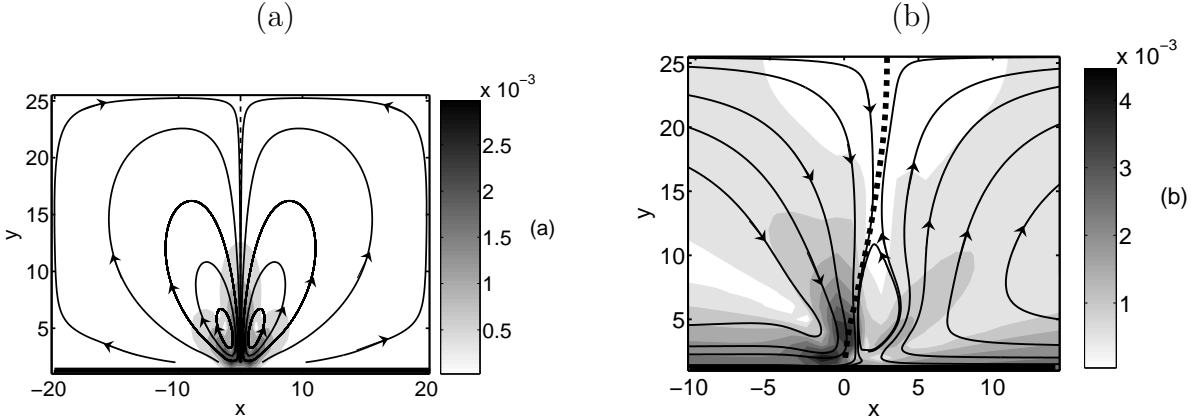


Figure 6: (a) The flow lines in the bottom half of  $100 \times 50$  lattice sites. The wall is marked with a solid line at  $y = 0$  and the interface with a dashed line at  $x = 0$ . The flow circulates around the lattice and is induced by the stresses at the three-phase contact point. (b) Flow lines in the comoving frame for flow velocity  $v_x = 2.73 \times 10^{-3}$ . The grey scale gives the magnitude of the flow velocity in both plots.

pressure near the corner node. Instead it induces a flow where particles flow towards the corner node along the interface and away from it along the wall.

Figure 6 shows how this works. Here the solid wall is neutrally wetting. This should recover an immobile flat interface. However due to spurious currents, a well-known phenomenon in LB interface models, the fluid is not at rest. Figure 6a shows the resulting flow pattern. The uncompensated stress at the three-phase contact point induces a circular flow pattern. In Figure 6b we show the flow pattern in the comoving frame with the average fluid velocity. This pattern is reminiscent of a rolling motion as presented in several classical models.

Further work shows that these flow patterns are independent of the net translational velocity of the interface. In other words, they are superimposed on any bulk flow. This explains how the contact line moves while keeping its shape constant. The circulation allows for rolling motion over the solid surface. Away from the interface we have the usual parabolic flow profile. As we move closer to the interface the flow profile becomes progressively flatter. Hence at the center of a capillary tube the interface appears rigid to the fluid and moves as a plug with constant velocity. Close to the walls, however, the viscous stresses increase and the interface is deformed. This forces the dynamic contact angle  $\theta_{\text{dyn}}$  to deviate from  $\theta_a$ . This change is linearly proportional to the capillary number. The proportionality factor of this change is however model-dependent. In slip models the proportionality factor depends on the slip length. In the LB model, the uncompensated stress component at the three-phase contact point induces a flow associated with a viscous length scale, which in turn derives from the microdynamics. Of course, slip lengths associated with real fluids are not viscous in origin. The main point, however, is that the uncompensated stresses in our LB model result in a moving contact-line phenomenology indistinguishable from real fluids.

## 3 Planned Activities

No further activities are planned.

## 4 Information Access

This project has resulted in three papers. Two are already published:

- Latva-Kokko, M. and Rothman, D. H., “Diffusion properties of gradient-based lattice Boltzmann models of immiscible fluids,” *Physical Review E* **71**, 056702, May 2005.
- Latva-Kokko, M. and Rothman, D. H., “Static contact angle in lattice-Boltzmann models of immiscible fluids,” *Physical Review E* **72**, 046701, October 2005.

The third paper is currently in review:

- Latva-Kokko, M. and Rothman, D. H., “Scaling of dynamic contact angles in a lattice-Boltzmann model,” submitted to *Physical Review Letters*, April 2006.